WEIZMANN INSTITUTE OF SCIENCE

Searches for new phenomena in final states with leptons and jets using the ATLAS detector

DISSERTATION

submitted in partial fulfilment of the requirements
for the degree of

DOCTOR OF PHILOSOPHY

in Physics

by

Roy Schimmel Brener

Month, 2026

TABLE OF CONTENTS

LIST OF FIGURES

LIST OF TABLES

ACKNOWLEDGMENTS

I would like to thank...

(You must acknowledge grants and other funding assistance.

You may also acknowledge the contributions of professors and friends.

You also need to acknowledge any publishers of your previous work who have given you permission to incorporate that work into your dissertation. See Section 3.2 of the UCI Thesis and Dissertation Manual.)

ABSTRACT OF THE DISSERTATION

Searches for new phenomena in final states with leptons and jets using the ATLAS detector

By

Roy Schimmel Brener

Weizmann Institute of Science, Month, 2026

The abstract of your contribution goes here.

Chapter 1

The Standard Model

Employing the gifts of Quantum Field Theory (QFT), a mathematical framework combines Quantum Mechanics (QM) and special relativity to describe the behaviour of fundamental particles and their interactions. The Standard Model (SM) is a QFT that codifies matter particles and force carriers within a unified theoretical structure. It describes three of the four known forces in the Universe: the electromagnetic, weak, and strong interactions. The SM has been remarkably successful in providing accurate predictions for a wide range of phenomena in particle physics, which have been confirmed by numerous experimental results.

This chapter gives and overview of the SM, starting from its underlying symmetries, followed by a description of its matter content and fundamental interactions. The chapter then introduces the quantum fields that represent particles with different spins, and discusses the Higgs mechanism responsible for electroweak symmetry breaking and mass generation. Finally, the chapter highlights limitations of the SM, motivating searches for physics beyond its framework.

This is an example using the LaTeX template for UCI theses and dissertation documents [24]. Figure 1.1 is just for illustration purposes, as is Table **??**.

```
#include <iostream>
int main(int argc, char** argv) {
  std::cout << "Hello World." << std::endl;
  return 0;
}
```

Figure 1.1: Example source code.

1.1 Symmetries and Conservation Laws

1.1.1 Spacetime Symmetries and Noether's Theorem

Any relativistic quantum field theory must be invariant under the Poincaré group, which combines spacetime translations and Lorentz transformations (rotations and boosts). We write this as

$$\mathcal{P} = \mathbb{R}^{1,3} \rtimes \mathrm{SO}(1,3), \tag{1.1}$$

where $\mathbb{R}^{1,3}$ denotes spacetime translations and $\mathrm{SO}(1,3)$ the Lorentz group. The semi-direct product $\rtimes$ reflects that these operations don't commute: a Lorentz transformation followed by a translation differs from the reverse order, since the transformation rotates the direction of translation in spacetime.

Invariance under spacetime translations means physics is the same everywhere and at all times. Lorentz invariance ensures all inertial observers agree on the fundamental laws. These symmetries connect directly to conservation laws through Noether's theorem: every continuous symmetry of the action corresponds to a conserved quantity.

Consider an action

$$S = \int d^4x \, \mathcal{L}(\phi, \partial_\mu \phi), \tag{1.2}$$

where $\mathcal{L}$ is the Lagrangian density and ϕ represents the fields. If the action is invariant under a continuous field transformation

$$\phi(x) \to \phi(x) + \delta\phi(x). \tag{1.3}$$

then there exists a conserved current j^μ satisfying

$$\partial_\mu j^\mu = 0. \tag{1.4}$$

This implies the charge

$$Q = \int d^3x\, j^0(x), \tag{1.5}$$

is constant in time. Time translation invariance yields energy conservation, spatial translations give momentum conservation, and rotations ensure angular momentum is conserved.

1.1.2 Internal Symmetries and Gauge Fields

Beyond spacetime symmetries, fields can have internal symmetries—transformations that act on the fields themselves while leaving coordinates unchanged. Consider a complex scalar field with Lagrangian

$$\mathcal{L} = \partial_\mu \phi^\dagger \partial^\mu \phi - m^2 \phi^\dagger \phi, \tag{1.6}$$

which describes a complex scalar field $\phi(x)$. This is invariant under the global phase transformation

$$\phi(x) \to e^{i\alpha} \phi(x), \tag{1.7}$$

where α is constant everywhere. This is a global $U(1)$ symmetry—the group of unit complex numbers under multiplication. Noether's theorem gives the conserved current

$$j^\mu = i\left(\phi^\dagger \partial^\mu \phi - \partial^\mu \phi^\dagger \phi\right), \tag{1.8}$$

with $\partial_\mu j^\mu = 0$. The conserved charge represents particle number or electric charge depending on context. This symmetry is Abelian: transformations commute.

The key step is promoting this to a local symmetry where α depends on position,

$$\phi(x) \to e^{i\alpha(x)} \phi(x). \tag{1.9}$$

However, the Lagrangian in Eq. (1.6) fails to be invariant under this transformation, because derivatives of ϕ produce unwanted terms involving $\partial_\mu \alpha(x)$.

Restoring invariance requires introducing a new vector field $A_\mu(x)$, the gauge field, and replacing ordinary derivatives with covariant derivatives,

$$D_\mu = \partial_\mu + ieA_\mu, \tag{1.10}$$

where e is a coupling constant. Under the local transformation, the gauge field must transform as $A_\mu \to A_\mu - (1/e)\partial_\mu \alpha(x)$ to compensate for the derivative terms. This procedure—demanding local gauge invariance—naturally produces quantum electrodynamics (QED), where A_μ is identified with the photon field and e with the electric charge.

The profound lesson is that requiring local symmetry inevitably introduces interaction: the gauge field mediates forces between charged particles. This gauge principle, applied to more elaborate symmetry groups, generates the complete structure of the Standard Model.

Non-Abelian Gauge Symmetries

The gauge principle extends beyond the Abelian $U(1)$ case to non-Abelian groups, where multiple symmetry generators do not commute with one another. These non-Abelian symmetries lead to richer physics: the gauge fields themselves carry the charges associated with the symmetry, leading to self-interactions absent in QED.

In the Standard Model, the full gauge group is

$$SU(3)_{\mathrm{C}} \times SU(2)_{\mathrm{L}} \times U(1)_{\mathrm{Y}}, \tag{1.11}$$

where $SU(3)_{\mathrm{C}}$ describes the strong interactions between quarks (quantum chromodynamics), $SU(2)_{\mathrm{L}}$ governs the weak interactions acting on left-handed fermions, and $U(1)_{\mathrm{Y}}$ represents the hypercharge interaction. The $SU(3)$ and $SU(2)$ factors are non-Abelian, resulting in the self-interactions of gluons and weak bosons that distinguish these forces from electromagnetism.

The complete realization of this gauge structure requires additional elements, particularly spontaneous symmetry breaking through the Higgs mechanism, which generates masses for the weak gauge bosons while preserving the underlying gauge invariance. These aspects, along with the detailed structure of fermion representations under the gauge group, will be developed in the sections that follow.

1.2 Matter Content and Fundamental Interactions

The Standard Model (SM) of particle physics is a relativistic quantum field theory defined by the fundamental gauge group

$$\mathcal{G}_{\rm SM} = SU(3)_{\rm C} \times SU(2)_{\rm L} \times U(1)_{\rm Y}. \tag{1.12}$$

The fundamental fields are classified by their transformation properties (representations) under these three factor groups, which dictates their interactions:

- $SU(3)_{\rm C}$ (Color): Governs the strong force (QCD).
- $SU(2)_{\rm L}$ (Weak Isospin): Governs the weak force.
- $U(1)_{\rm Y}$ (Hypercharge): Governs the electromagnetic interaction (after symmetry breaking).

1.2.1 The Gauge Boson Sector

The gauge fields (bosons) mediate the forces and arise directly from the local gauge invariance requirement. The number of gauge fields is equal to the dimension (number of generators) of the associated symmetry group:

- $U(1)_{\rm Y}$: 1 generator $\implies$ 1 gauge field (B_μ).
- $SU(2)_{\rm L}$: $2^2 - 1 = 3$ generators $\implies$ 3 gauge fields (W^a_μ, $a = 1, 2, 3$).
- $SU(3)_{\rm C}$: $3^2 - 1 = 8$ generators $\implies$ 8 gauge fields (G^A_μ, $A = 1, \ldots, 8$).

In total, the SM features 12 gauge bosons. The kinetic term for the non-Abelian gauge fields is given by the Yang-Mills Lagrangian density:

$$\mathcal{L}_{\rm YM} = -\frac{1}{4} F^A_{\mu\nu} F^{\mu\nu,A}, \tag{1.13}$$

where the field strength tensor $F^A_{\mu\nu}$ includes terms representing the crucial self-interaction of the non-Abelian gauge bosons (gluons and W/Z fields).

1.2.2 The Fermion Sector (Matter)

The matter content consists of 12 fundamental fermions (and their antiparticles), organized into three generations. Fermions are introduced as left-handed (ψ_{L}) and right-handed (ψ_{R}) Weyl spinors. This distinction is vital, as the $SU(2)_{\mathrm{L}}$ weak interaction only couples to left-handed fields.

The representation of each field under $\mathcal{G}_{\mathrm{SM}}$ determines its charge and interaction. We list the fields for a single generation (electron/neutrino and up/down quarks) in Table 1.1.

Table 1.1: Fermionic Content of the Standard Model (One Generation)

Field Name	**Symbol**	$\mathbf{SU(3)_C}$	$\mathbf{SU(2)_L}$	$\mathbf{U(1)_Y}$	**Total Components**
Lepton Doublet	L_{L}	**1** (Singlet)	**2** (Doublet)	$-1/2$	4
Electron Singlet	e_{R}	**1** (Singlet)	**1** (Singlet)	-1	2
Quark Doublet	Q_{L}	**3** (Triplet)	**2** (Doublet)	$+1/6$	$3 \times 2 = 6$
Up-type Singlet	u_{R}	**3** (Triplet)	**1** (Singlet)	$+2/3$	$3 \times 1 = 3$
Down-type Singlet	d_{R}	**3** (Triplet)	**1** (Singlet)	$-1/3$	$3 \times 1 = 3$

The physical electric charge Q is derived from the weak isospin third component (T_3) and the hypercharge (Y) via the **Gell-Mann–Nishijima Relation** (in the context of electroweak theory):

$$Q = T_3 + Y. \tag{1.14}$$

Explicit Field Components and Charges (First Generation)

- **Lepton Doublet (L_{L}):**

$$L_{\mathrm{L}} = \begin{pmatrix} \nu_e \\ e \end{pmatrix}_{\mathrm{L}}, \quad T_3 = \begin{pmatrix} +1/2 \\ -1/2 \end{pmatrix}, \quad Y = -1/2.$$

  - $\nu_{e,\mathrm{L}}$ (Neutrino): $Q = +1/2 + (-1/2) = 0$.
  - e_{L} (Electron): $Q = -1/2 + (-1/2) = -1$.

- **Quark Doublet (Q_{L}):** (3 color components for each element)

$$Q_{\mathrm{L}} = \begin{pmatrix} u \\ d \end{pmatrix}_{\mathrm{L}}, \quad T_3 = \begin{pmatrix} +1/2 \\ -1/2 \end{pmatrix}, \quad Y = +1/6.$$

- u_{L} (Up Quark): $Q = +1/2 + 1/6 = +2/3$.
- d_{L} (Down Quark): $Q = -1/2 + 1/6 = -1/3$.

The right-handed fields (e_{R}, u_{R}, d_{R}) are $SU(2)_{\mathrm{L}}$ singlets, thus $T_3 = 0$, and their charges are simply $Q = Y$.

1.2.3 The Higgs Sector

The model requires a complex scalar field, the Higgs doublet, Φ, to implement electroweak symmetry breaking (EWSB).

Field Name	**Symbol**	$\mathbf{SU(3)_C}$	$\mathbf{SU(2)_L}$	$\mathbf{U(1)_Y}$
Higgs Doublet	Φ	**1** (Singlet)	**2** (Doublet)	$+1/2$

The Higgs field facilitates two essential mechanisms:

1. **EWSB:** Spontaneous symmetry breaking via the Higgs field breaks $\mathcal{G}_{\mathrm{EW}} \to U(1)_{\mathrm{EM}}$, thereby generating masses for the $W^{\pm}$ and Z^0 bosons.
2. **Fermion Masses:** The Higgs field couples to fermions via Yukawa couplings, which, after EWSB, give mass to the fundamental matter particles.

The detailed implementation of EWSB and mass generation will be covered in the following sections.

1.3 Spin-0, Spin-1/2, and Spin-1 Quantum Fields

1.4 The Higgs Mechanism and Electroweak Symmetry Breaking

1.5 Limitations of the Standard Model

Chapter 2

Beyond the Standard Model

Introductory words about needing for physics beyond the SM. Note this chapter is not exhaustive, but only shows some of the motivations that particulalrly relate to my thesis work.

2.1 Dark Matter

2.2 Flavour anomalies

2.3 Hierarchy problem

Chapter 3

Experimental Apparatus

Words about CERN, LHC and ATLAS.

3.1 The Large Hadron Collider

3.2 The ATLAS Detector

3.3 The New Small Wheel Upgrade

Chapter 4

Objects Reconstruction

Fusce mauris. Vestibulum luctus nibh at lectus. Sed bibendum, nulla a faucibus semper, leo velit ultricies tellus, ac venenatis arcu wisi vel nisl. Vestibulum diam. Aliquam pellentesque, augue quis sagittis posuere, turpis lacus congue quam, in hendrerit risus eros eget felis. Maecenas eget erat in sapien mattis porttitor. Vestibulum porttitor. Nulla facilisi. Sed a turpis eu lacus commodo facilisis. Morbi fringilla, wisi in dignissim interdum, justo lectus sagittis dui, et vehicula libero dui cursus dui. Mauris tempor ligula sed lacus. Duis cursus enim ut augue. Cras ac magna. Cras nulla. Nulla egestas. Curabitur a leo. Quisque egestas wisi eget nunc. Nam feugiat lacus vel est. Curabitur consectetuer.

4.1 Tracks and Primary Vertices

Fusce mauris. Vestibulum luctus nibh at lectus. Sed bibendum, nulla a faucibus semper, leo velit ultricies tellus, ac venenatis arcu wisi vel nisl. Vestibulum diam. Aliquam pellentesque, augue quis sagittis posuere, turpis lacus congue quam, in hendrerit risus eros eget felis. Maecenas eget erat in sapien mattis porttitor. Vestibulum porttitor. Nulla facilisi. Sed a turpis eu lacus commodo facilisis. Morbi fringilla, wisi in dignissim interdum, justo lectus sagittis dui, et vehicula libero dui cursus dui. Mauris tempor ligula sed lacus. Duis cursus enim ut augue. Cras ac magna. Cras nulla. Nulla egestas. Curabitur a leo. Quisque egestas wisi eget nunc. Nam feugiat lacus vel est. Curabitur consectetuer.

4.2 Electrons

Fusce mauris. Vestibulum luctus nibh at lectus. Sed bibendum, nulla a faucibus semper, leo velit ultricies tellus, ac venenatis arcu wisi vel nisl. Vestibulum diam. Aliquam pellentesque, augue quis sagittis posuere, turpis lacus congue quam, in hendrerit risus eros eget felis. Maecenas eget erat in sapien mattis porttitor. Vestibulum porttitor. Nulla facilisi. Sed a turpis eu lacus commodo facilisis. Morbi fringilla, wisi in dignissim interdum, justo lectus sagittis dui, et vehicula libero dui cursus dui. Mauris tempor ligula sed lacus. Duis cursus enim ut augue. Cras ac magna. Cras nulla. Nulla egestas. Curabitur a leo. Quisque egestas wisi eget nunc. Nam feugiat lacus vel est. Curabitur consectetuer.

4.3 Photons

Fusce mauris. Vestibulum luctus nibh at lectus. Sed bibendum, nulla a faucibus semper, leo velit ultricies tellus, ac venenatis arcu wisi vel nisl. Vestibulum diam. Aliquam pellentesque, augue quis sagittis posuere, turpis lacus congue quam, in hendrerit risus eros eget felis. Maecenas eget erat in sapien mattis porttitor. Vestibulum porttitor. Nulla facilisi. Sed a turpis eu lacus commodo facilisis. Morbi fringilla, wisi in dignissim interdum, justo lectus sagittis dui, et vehicula libero dui cursus dui. Mauris tempor ligula sed lacus. Duis cursus enim ut augue. Cras ac magna. Cras nulla. Nulla egestas. Curabitur a leo. Quisque egestas wisi eget nunc. Nam feugiat lacus vel est. Curabitur consectetuer.

4.4 Muons

Fusce mauris. Vestibulum luctus nibh at lectus. Sed bibendum, nulla a faucibus semper, leo velit ultricies tellus, ac venenatis arcu wisi vel nisl. Vestibulum diam. Aliquam pellentesque, augue quis sagittis posuere, turpis lacus congue quam, in hendrerit risus eros eget felis. Maecenas eget erat in sapien mattis porttitor. Vestibulum porttitor. Nulla facilisi. Sed a turpis eu lacus commodo facilisis. Morbi fringilla, wisi in dignissim interdum, justo lectus sagittis dui, et vehicula libero dui cursus dui. Mauris tempor ligula sed lacus. Duis cursus enim ut augue. Cras ac magna. Cras nulla. Nulla egestas. Curabitur a leo. Quisque egestas

wisi eget nunc. Nam feugiat lacus vel est. Curabitur consectetuer.

4.4.1 Run2 muons

4.4.2 Run3 muons

Fusce mauris. Vestibulum luctus nibh at lectus. Sed bibendum, nulla a faucibus semper, leo velit ultricies tellus, ac venenatis arcu wisi vel nisl. Vestibulum diam. Aliquam pellentesque, augue quis sagittis posuere, turpis lacus congue quam, in hendrerit risus eros eget felis. Maecenas eget erat in sapien mattis porttitor. Vestibulum porttitor. Nulla facilisi. Sed a turpis eu lacus commodo facilisis. Morbi fringilla, wisi in dignissim interdum, justo lectus sagittis dui, et vehicula libero dui cursus dui. Mauris tempor ligula sed lacus. Duis cursus enim ut augue. Cras ac magna. Cras nulla. Nulla egestas. Curabitur a leo. Quisque egestas wisi eget nunc. Nam feugiat lacus vel est. Curabitur consectetuer.

4.5 Jets

Fusce mauris. Vestibulum luctus nibh at lectus. Sed bibendum, nulla a faucibus semper, leo velit ultricies tellus, ac venenatis arcu wisi vel nisl. Vestibulum diam. Aliquam pellentesque, augue quis sagittis posuere, turpis lacus congue quam, in hendrerit risus eros eget felis. Maecenas eget erat in sapien mattis porttitor. Vestibulum porttitor. Nulla facilisi. Sed a turpis eu lacus commodo facilisis. Morbi fringilla, wisi in dignissim interdum, justo lectus sagittis dui, et vehicula libero dui cursus dui. Mauris tempor ligula sed lacus. Duis cursus enim ut augue. Cras ac magna. Cras nulla. Nulla egestas. Curabitur a leo. Quisque egestas wisi eget nunc. Nam feugiat lacus vel est. Curabitur consectetuer.

4.6 Missing Transverse Momentum

Fusce mauris. Vestibulum luctus nibh at lectus. Sed bibendum, nulla a faucibus semper, leo velit ultricies tellus, ac venenatis arcu wisi vel nisl. Vestibulum diam. Aliquam pellentesque, augue quis sagittis posuere, turpis lacus congue quam, in hendrerit risus eros eget felis.

Maecenas eget erat in sapien mattis porttitor. Vestibulum porttitor. Nulla facilisi. Sed a turpis eu lacus commodo facilisis. Morbi fringilla, wisi in dignissim interdum, justo lectus sagittis dui, et vehicula libero dui cursus dui. Mauris tempor ligula sed lacus. Duis cursus enim ut augue. Cras ac magna. Cras nulla. Nulla egestas. Curabitur a leo. Quisque egestas wisi eget nunc. Nam feugiat lacus vel est. Curabitur consectetuer.

Chapter 5

Toolkit for HEP Searches

Words about common tools used in HEP searches, such as bkg. estimation, statistical inference, etc.

5.1 Analysis Strategies

5.2 Background Estimation Techniques

5.3 Systematic Uncertainties

5.4 Statistical Inference

5.5 something else

5.6 another thing

5.7 yet another thing

Chapter 6

Search for New Physics in ℓj Final States at $\sqrt{s} = 13.6$ TeV

6.1 Introduction

The hierarchy problem [22] is a key question in high-energy physics as it addresses the limits of the Standard Model (SM) in conjunction with quantum gravity. The Planck Mass, $M_{\mathrm{Pl}} = \sqrt{\hbar c/G} \sim \mathcal{O}(10^{19})$ GeV, marks the boundary between energy scales where the Standard Model may remain valid and those where gravitational effects become significant. The Higgs mass, m_h, measured [6] at 125 GeV, is extremely small compared to the Planck mass. Furthermore, one expects the Higgs Vacuum Expectation Value (VEV) to be sensitive to the top mass, m_t, and other heavy states thereby making the gap between m_h and M_{Pl} even more pronounced. This disparity suggests that the SM may be valid only up to a certain scale, Λ, above which New Physics (NP) is expected to emerge. Two classes of models are typically concerned with compactifying extra dimensions (EDs) that are introduced in solutions to the hierarchy problem: the Randall-Sundrum (RS) model [25] and the Arkani-Hamed, Dimopoulos, Dvali (ADD) model [15, 14]. The former refers to a model with a single extra dimension, RS1, which is the only one within RS allowing for QBHs. The latter can have an arbitrary number of EDs. Both suggest manifestations of quantum gravity accessible at LHC energies. One theoretical object introduced within this paradigm is the Quantum Black Hole (QBH) [20, 23, 17]. QBHs are predicted in low-energy quantum gravity models [25, 15, 14], which address the hierarchy problem by lowering the scale of quantum

gravity, M_{D}, from M_{Pl} to the TeV region, where both gravity and quantum effects come into play.

In ADD, the gravitational field is permitted to propagate in $4+n$ dimensions, whilst keeping all SM fields localised in the usual four-dimensional spacetime. Here, the EDs are large and flat and their size leads to a reduction in the effective gravitational strength at small scale. Conversely, RS1 proposes a scenario, where a single curved extra dimension is where gravity also propagates. Its curvature, determined by a warp factor, results in an exponential hierarchy between the Planck and electroweak scales, thereby addressing the hierarchy problem. These models introduce postulates which include conservation of total angular momentum, colour and electric charge in the production and decay of QBHs [20]. Unlike semi-classical black holes [13], which undergo thermal decay into multi-particle final states via Hawking radiation [9, 2, 26, 28], QBHs with threshold mass, $M_{\mathrm{th}} \sim M_{\mathrm{D}}$, are predicted to predominantly decay into two-particle final states.

Measurements thus far have constrained $M_{\mathrm{th}} \sim M_{\mathrm{D}} \gtrsim \mathcal{O}(10)$ TeV, such that QBHs can be searched for at LHC energies. Although strong-gravity interactions are expected to conserve angular momentum, electric charge and colour, it is unclear whether they conserve SM global symmetries like baryon and lepton number. Despite baryon number violation being small in four-dimensional M_{Pl}-scale gravity [20], in TeV-scale gravity with EDs the size of this violation is less constrained and hence may bear an impact on observables. Therefore, a search for QBH production which violates SM global symmetries may help test TeV-scale gravity behaviour.

The QBH production mechanisms can be described as a set of 2-to-2 scattering processes, considering only states that decay to final states involving a single lepton,

$$uu \to \bar{d}\ell^+, ud \to \bar{u}\ell^+, \bar{d}\bar{d} \to d\ell^+, \tag{6.1}$$

and charge conjugates thereof, where u and d denote up- and down-quarks of all flavours, respectively, and ℓ is a charged lepton. The possible decays depend on the QBH state, these states are described using $QBH^{\text{Electric Charge}}_{\text{Inital Quarks/Gluons}}$, Qstate, and Istate. Qstate refers to three times this electric charge and Istate refers to initial state, which indicates the number of gluons in the intial state, this is 0 for all states considered as they are quark only [19]. Considering only QBHs decaying to lepton-quark pairs, the relevant six QBH states are: $QBH^{\pm\frac{4}{3}}_{uu/\overline{u}\overline{u}}$, $QBH^{\pm\frac{2}{3}}_{\overline{d}\overline{d}/dd}$, $QBH^{\pm\frac{1}{3}}_{ud/\overline{u}\overline{d}}$. As a matter of analysis choice, τ-leptons are excluded.

The study of QBH to τ + jet decay would require the combination of the possible decay modes of the τ lepton, due to this complication this, and other exotics analyses, consider these as seperate searches.

Previously, ATLAS searched for QBHs in lepton+jet final states on two occasions, first at a centre-of-mass energy of $\sqrt{s} = 8$ TeV with full Run1 proton-proton collision data [5]. The second search was conducted with full Run2 data at a centre-of-mass energy of $\sqrt{s} =$ 13.0 TeV and excluded QBH with $M_{\text{th}} = 9.2$ (6.8) TeV for the ADD (RS) models [12]. QBHs have also been searched in dijet and dilepton final states by ATLAS [7, 1, 10] and CMS [27, 29] at $\sqrt{s} = 13.0$ TeV LHC energy. Searches in photon+jet were conducted by ATLAS at $\sqrt{s} = 8$ TeV [4] and twice at $\sqrt{s} = 13.0$ TeV, with 3.2 fb^{-1} [8] and 36.7 fb^{-1} [3]; and by CMS [30] at $\sqrt{s} = 13.0$ TeV with 138 fb^{-1}. Searches for QBHs in different final states complement one another, as the quantum states considered are different [21]. Amongst these, searches in the lepton+jet final state set the highest exclusion limits, reaching greater M_{th} values than all other final states. This makes them particularly powerful while still providing complementary coverage to other search channels. At equal M_{th} ranges, QBH searches in lepton+jet final states are generally less sensitive than those obtained by searches in dijet final states. Conversely, limits from lepton+jet searches are stronger than those with photon+jet and dilepton final states.

6.2 Executive Summary

A summary of key analysis points is given below

- **Physics target**: search for signatures of QBHs in electron+jet and muon+jet final states.
- **Observable**: invariant mass of the lepton-jet system, $m_{\ell j}$; statistical analysis in bins of $m_{\ell j}$.
- **Strategy**: signal and background are estimated from MC using a set of event generators. In the $e + j$ channel, the non-prompt/multijet ("fake" electrons) background is estimated using a data-driven approach. The search is performed in a wide signal region starting at 3 TeV, with QBH threshold mass range of 6–10.5 TeV.

- **Collision dataset**: Run3 data collected by ATLAS between 2022–2024 at $\sqrt{s}$ = 13.6 TeV with 165.4 fb^{-1}.

6.2.1 Context and Motivation

The LHC is currently operating at Run3 running period, where its centre-of-mass energy is $\sqrt{s} = 13.6$ TeV [11], a modest increase of 0.6 TeV with respect to Run2. The total integrated luminosity recorded by ATLAS thus far is 165 fb^{-1} and it includes proton-proton collision data recorded during 2022–2024. Partial Run 3 (2022-2024) compared to Run 2 therefore has a slightly higher centre of mass energy and more data. Both of these benefit QBH searches. QBH production cross-sections increase significantly with $\sqrt{s}$, such that even a moderate rise in the collider energy would induce considerably higher σ(QBH) [18]. They are one of the very few signals (if not the only) which would considerably benefit from this small energy increase. To probe this expected increase, production cross sections of QBHs generated with the event generator `QBH v3.02` [19], which follow the six quantum states noted in Section **??**, are computed for $\sqrt{s} = 13.0$ and 13.6 TeV for the ADD and RS models in the 3–9 TeV range, as shown in FIG. 6.1.

The gain becomes gradually more pronounced as M_{th} grows. By increasing $\sqrt{s}$ to 13.6 TeV, σ(QBH) increases by $\sim$ 12% to above 250% for $3 \leq M_{\text{th}} \leq 9$ TeV. The addition of the expected integrated luminosity of 2024 would likely induce a gain in exclusion power for both models, at $\mathcal{O}(500)$ GeV. Therefore, the motivation to include QBH signals with a partial Run3 dataset is clear.

An early Run3 search with leptons and jets in ATLAS is also highly motivated from a completely experimental point of view. Apart from software-based upgrades to the data and simulation processing, storage and availability, during the 2019–2022 shutdown the ATLAS detector underwent several major upgrades that are expected to effect the reconstruction of leptons and jets. Apart from re-configuring the combined-performance analyses into object-specific reconstruction quality, it is also desired to perform early searches where a full set of recommended quality requirements are applied on different objects (electrons, muons, jets, $E_{\text{T}}^{\text{miss}}$) used within them. Finally, towards Run3, ATLAS has made several important upgrades to its data processing software `Athena` [16], key amongst which are support for multi-threaded event processing, quicker tracking reconstruction and most importantly, re-

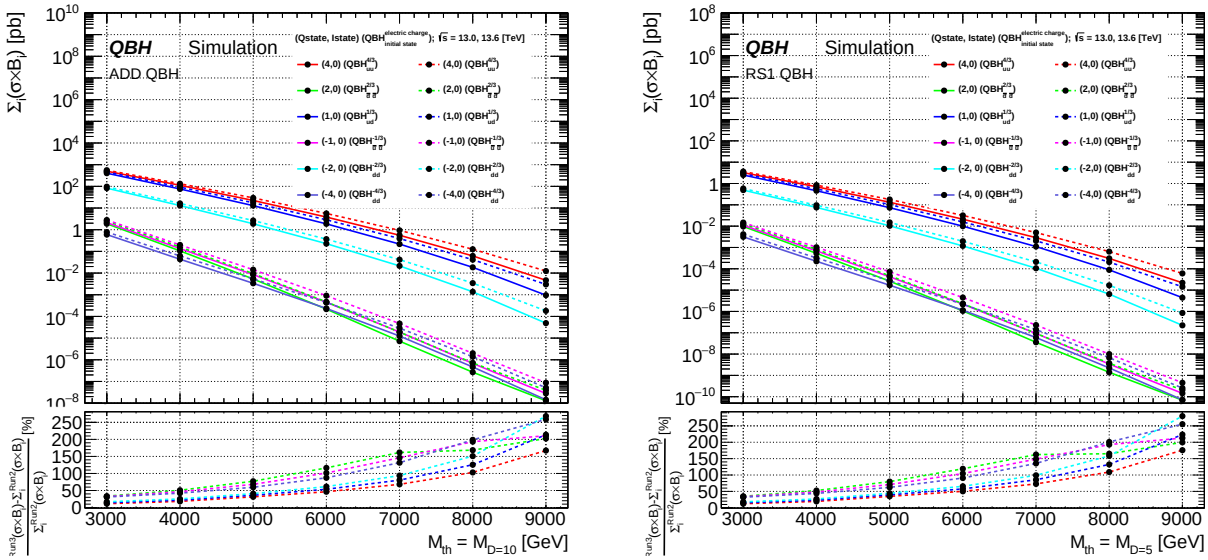

Figure 6.1: Summed production cross sections times branching fractions of QBHs at different threshold masses, M_{th}, for ADD (left) and RS (right) models with $n = 6$ and $n = 1$ extra dimensions, respectively. The colours indicate all possible quantum states of the QBH that can decay to a ℓj final state. Solid and dashed lines indicate the two $\sqrt{s}$ values of the LHC centre-of-mass energy, 13.0 TeV and 13.6 TeV for Run2 and Run3, respectively. The bottom pane shows the relative increase (%) in cross section, calculated as the difference between the Run 3 and Run 2 values, divided by the Run 2 value. This represents the gain due to the higher $\sqrt{s}$.

construction and simulation of the New Small Wheel (NSW). Therefore, it is desired to consolidate new software updates to early Run3 analyses to test recent improvements.

6.2.2 Analysis Strategy

QBHs decaying to lepton-quark pairs are searched for. The two-body decay is reconstructed from exactly one energetic electron or muon and one energetic jet. High-p_{T} requirements are set on the leading lepton and jet, in addition to geometrical cuts, which select back-to-back two-body decays. Electron, muons, jets and $E_{\text{T}}^{\text{miss}}$ are the objects used and whose quality requirements are set by data preparations. The ntuples are filtered such that each event must contain one or two baseline leptons as well as at least one signal jet, all with transverse momentum above 150 GeV. The discriminant used is the invariant mass of the leading signal lepton and signal jet, $m_{\ell j}$, which is required to be above 1.0 TeV — the lower bound of the analysis regions. This analysis focuses on final states containing a light lepton, electron or

muon, with potential contamination from τ decays and other QBH states misidentified as $e + j$ or $\mu + j$ expected to be minimal. Their contribution is not explicitly estimated but is expected to have a negligible impact on the results.

The analysis strategy is similar for the two lepton flavours, except for the fact that in the $e + j$ channel, the multijet background is included whereas in the $\mu + j$ channel it is nearly negligible. This is due to the fact it is more likely for a jet to be misidentified as an electron than as a muon. To that end, in the electron channel it is estimated from data and from dijet Monte Carlo (MC) in the muon channel. The analysis region definitions and cuts are shown schematically in FIG. 6.2.

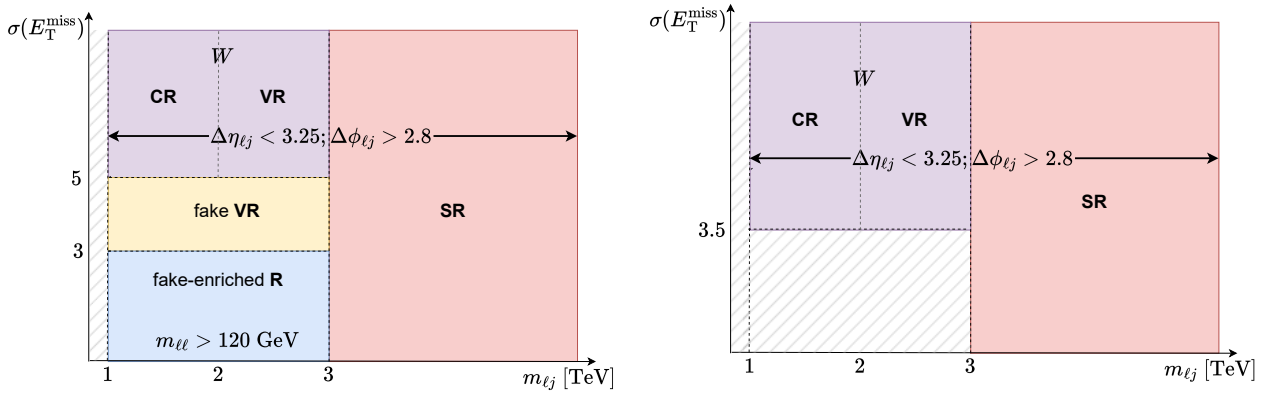

Figure 6.2: Analysis regions for the $e + j$ channel (left) and $\mu + j$ channel (right) defined along the x-, y-axis qualitatively representing $m_{\ell j}$, $\sigma(E_{\mathrm{T}}^{\mathrm{miss}})$, respectively. Control, validation regions for the leading backgrounds W+jets and fake-electrons are shown. The Z+jets background is controlled equivalently amongst the two channels, in $m_{\ell j}$ ranges and a requirement for a second baseline lepton as well as for the dilepton invariant mass to be around the Z peak. The channels differ due to the need to estimate the fake-electron background in the $e + j$ channel. The hashed regions are excluded in the analysis. The analysis lower bound is set at $m_{\ell j} = 1.0$ TeV to focus on events with very-high p_{T} leptons and jets, restrict the phase space to the extreme kinematic region, filter out lower-mass events and maintain sufficient phase-space between 1 and 3 TeV for control and validation of leading backgrounds below and adjacent to the signal region beginning at 3 TeV.

The analysis regions illustrated in FIG. 6.2 differ between the $e+j$ and $\mu+j$ channels in that the former includes the fake-electron background as a controlled and validated background source. The $e + j$ fake control region requires $\sigma(E_{\mathrm{T}}^{\mathrm{miss}}) < 3.0$ to suppress contributions from W+jets events, whereas the fake VR sets $3.0 < \sigma(E_{\mathrm{T}}^{\mathrm{miss}}) < 5.0$ as a middle ground between a fake-enriched region and W+jets contamination. To maintain orthogonality between these

regions, the W+jets CR (VR) begins at $\sigma(E_{\mathrm{T}}^{\mathrm{miss}}) = 5.0$. For the $\mu + j$ channel, a similar-but-simpler analysis strategy is devised, where the only backgrounds controlled and validated are W+jets and Z+jets. Lacking the need to estimate a fake-electron background from data in dedicated regions, the W+jets VR starts at an earlier value of $\sigma(E^{\mathrm{miss}}) = 3.5$.

The Z+jets CR (VR), equally defined between the electron and muon channels, is enriched by requiring the presence of a baseline lepton in addition to the signal lepton. The invariant dilepton mass must lie within 30 GeV away from m_Z, within the $[60, 120]$ GeV range. Other subdominant sources of background such as events from top decays and diboson processes each amount to less than 10% in the SR.

To enhance sensitivity in the SRs, angular cuts on the lepton-jet system are applied, selecting events where the lepton and jet are approximately back-to-back in the transverse plane while maintaining high signal efficiency. The azimuthal angle difference between the lepton and the jet, defined as $\Delta\phi_{\ell j} = |\phi_\ell - \phi_j|$, where ϕ_ℓ and ϕ_j are the azimuthal angles of the lepton and jet, respectively, quantifies their separation in the transverse plane. The pseudorapidity difference between the lepton and the jet, defined as $\Delta\eta_{\ell j} = |\eta_\ell - \eta_j|$, where η_ℓ and η_j are the pseudorapidities of the lepton and jet, measures their separation along the longitudinal direction. Cuts on these variables are applied as outlined in FIG. 6.2, and are implemented in both the SR and W+jets CRs/VRs.

Using a profile-likelihood fit, normalisation factors are derived for the W+jets and Z+jets background estimates, used to produce an Asimov dataset in the post-fit SR. Systematic uncertainties from detector simulation on the analysis objects, electrons, muons, jets and $E_{\mathrm{T}}^{\mathrm{miss}}$, as well as theoretical uncertainties on the PDF choice, QCD scales and others are considered as nuisance parameters in the fit. A limit on the signal strength, μ, calculated at each signal point is used to place exclusion limits on the QBH production cross-section times decay branching fraction.

Chapter 7

Search for New Resonances in $\ell\ell$ Final States at $\sqrt{s} = 13$ TeV

Chapter 8

Search for Periodic Signals in $ee/\gamma\gamma$ Final States at $\sqrt{s} = 13$ TeV

Chapter 9

Integration of Strips into the New Small Wheel Trigger System

Chapter 10

Concluding Remarks

Bibliography

[1] M. Aaboud et al. Search for new phenomena in different-flavour high-mass dilepton final states in pp collisions at $\sqrt{s} = 13$ Tev with the ATLAS detector. *Eur. Phys. J. C*, 76(10):541, 2016.

[2] M. Aaboud et al. Search for heavy particles decaying into top-quark pairs using lepton-plus-jets events in proton–proton collisions at $\sqrt{s} = 13$ TeV with the ATLAS detector. *Eur. Phys. J. C*, 78(7):565, 2018.

[3] M. Aaboud et al. Search for new phenomena in high-mass final states with a photon and a jet from *pp* collisions at $\sqrt{s} = 13$ TeV with the ATLAS detector. *Eur. Phys. J. C*, 78(2):102, 2018.

[4] G. Aad et al. Search for new phenomena in photon+jet events collected in proton–proton collisions at sqrt(s) = 8 TeV with the ATLAS detector. *Phys. Lett. B*, 728:562–578, 2014.

[5] G. Aad et al. Search for Quantum Black Hole Production in High-Invariant-Mass Lepton+Jet Final States Using *pp* Collisions at $\sqrt{s} = 8$ TeV and the ATLAS Detector. *Phys. Rev. Lett.*, 112(9):091804, 2014.

[6] G. Aad et al. Combined Measurement of the Higgs Boson Mass in *pp* Collisions at $\sqrt{s} =$ 7 and 8 TeV with the ATLAS and CMS Experiments. *Phys. Rev. Lett.*, 114:191803, 2015.

[7] G. Aad et al. Search for new phenomena in dijet mass and angular distributions from *pp* collisions at $\sqrt{s} = 13$ TeV with the ATLAS detector. *Phys. Lett. B*, 754:302–322, 2016.

[8] G. Aad et al. Search for new phenomena with photon+jet events in proton-proton collisions at $\sqrt{s} = 13$ TeV with the ATLAS detector. *JHEP*, 03:041, 2016.

[9] G. Aad et al. Search for strong gravity in multijet final states produced in pp collisions at $\sqrt{s} = 13$ TeV using the ATLAS detector at the LHC. *JHEP*, 03:026, 2016.

[10] G. Aad et al. Search for new resonances in mass distributions of jet pairs using 139 fb^{-1} of *pp* collisions at $\sqrt{s} = 13$ TeV with the ATLAS detector. *JHEP*, 03:145, 2020.

[11] G. Aad et al. The ATLAS Experiment at the CERN Large Hadron Collider: A Description of the Detector Configuration for Run 3, 5 2023.

[12] G. Aad et al. Search for quantum black hole production in lepton+jet final states using proton-proton collisions at $\sqrt{s} = 13$ TeV with the ATLAS detector, Feb 2024.

[13] L. A. Anchordoqui, J. L. Feng, H. Goldberg, and A. D. Shapere. Black holes from cosmic rays: Probes of extra dimensions and new limits on TeV scale gravity. *Phys. Rev. D*, 65:124027, 2002.

[14] I. Antoniadis, N. Arkani-Hamed, S. Dimopoulos, and G. R. Dvali. New dimensions at a millimeter to a Fermi and superstrings at a TeV. *Phys. Lett. B*, 436:257–263, 1998.

[15] N. Arkani-Hamed, S. Dimopoulos, and G. Dvali. The hierarchy problem and new dimensions at a millimeter. *Phys. Lett. B*, 429:263, 1998.

[16] R. Bielski and on behalf of the ATLAS Collaboration. Atlas high level trigger within the multi-threaded software framework athenamt. *Journal of Physics: Conference Series*, 1525(1):012031, apr 2020.

[17] X. Calmet, W. Gong, and S. D. H. Hsu. Colorful quantum black holes at the LHC. *Phys. Lett. B*, 668:20–23, 2008.

[18] D. M. Gingrich. Black hole cross-section at the large hadron collider. *Int. J. Mod. Phys. A*, 21:6653–6676, 2006.

[19] D. M. Gingrich. Monte Carlo event generator for black hole production and decay in proton-proton collisions. *Comput. Phys. Commun.*, 181:1917–1924, 2010.

[20] D. M. Gingrich. Quantum black holes with charge, colour, and spin at the LHC. *J. Phys. G*, 37:105008, 2010.

[21] D. M. Gingrich. Collider searches for nonperturbative low-scale gravity states. *Int. J. Mod. Phys. A*, 30(34):1530061, 2015.

[22] S. Koren. *New Approaches to the Hierarchy Problem and their Signatures from Microscopic to Cosmic Scales*. PhD thesis, UC, Santa Barbara, 2020.

[23] P. Meade and L. Randall. Black Holes and Quantum Gravity at the LHC. *JHEP*, 05:003, 2008.

[24] L. Otten. LaTeX template for thesis and dissertation documents at UC Irvine. https://github.com/lotten/uci-thesis-latex/, 2012.

[25] L. Randall and R. Sundrum. Large mass hierarchy from a small extra dimension. *Phys. Rev. Lett.*, 83:3370, 1999.

[26] A. M. Sirunyan et al. Search for black holes in high-multiplicity final states in proton-proton collisions at $\sqrt{s}$ =13 TeV. *Phys. Lett. B*, 774:279–307, 2017.

[27] A. M. Sirunyan et al. Search for new physics with dijet angular distributions in proton-proton collisions at $\sqrt{s} = 13$ TeV. *JHEP*, 07:013, 2017.

[28] A. M. Sirunyan et al. Search for black holes and sphalerons in high-multiplicity final states in proton-proton collisions at $\sqrt{s} = 13$ TeV. *JHEP*, 11:042, 2018.

[29] A. M. Sirunyan et al. Search for lepton-flavor violating decays of heavy resonances and quantum black holes to eμ final states in proton-proton collisions at $\sqrt{s} = 13$ TeV. *JHEP*, 04:073, 2018.

[30] A. Tumasyan et al. Search for resonances in events with photon and jet final states in proton-proton collisions at $\sqrt{s} = 13$ TeV. *JHEP*, 12:189, 2023.

Appendix A

Appendix Title

Supplementary material goes here. See for instance Figure A.1.

A.1 Lorem Ipsum

dolor sit amet, consectetur adipisicing elit, sed do eiusmod tempor incididunt ut labore et dolore magna aliqua. Ut enim ad minim veniam, quis nostrud exercitation ullamco laboris nisi ut aliquip ex ea commodo consequat. Duis aute irure dolor in reprehenderit in voluptate velit esse cillum dolore eu fugiat nulla pariatur. Excepteur sint occaecat cupidatat non proident, sunt in culpa qui officia deserunt mollit anim id est laborum.

"I am glad I was up so late,
for that's the reason I was up so early."
William Shakespeare (1564-1616), British dramatist, poet.
Cloten, in Cymbeline, act 2, sc. 3, l. 33-4.

Figure A.1: A deep quote.